

TEMPORAL GEOMETRIC CONSTRAINED BUNDLE ADJUSTMENT FOR THE AERIAL MULTI-HEAD CAMERA SYSTEM

Young-Jin Lee, Alper Yilmaz

Geodetic Science & Surveying, The Ohio State University, Columbus, Ohio, USA
(lee.3043, yilmaz.15)@osu.edu

KEY WORDS: multi-head camera, constrained bundle adjustment, temporal geometric constraint

ABSTRACT:

This paper describes the temporal geometric constrained bundle adjustment method for exterior orientations of individual images acquired from an aerial multi-head camera system without platform calibration parameters and navigation solutions. The aerial multi-head camera system provides a single synthetic image, which has large coverage, from precisely estimated exterior orientation parameters (EOP) of each image. The EOP of each image can be directly calculated from navigation solutions and platform geometric calibration parameters. However, if these values are not available for some reason, the EOP of each image can be estimated with control points. In this case, the geometric relationship between camera heads should be considered. Each camera of the multi-head camera system is tightly affixed to the platform; therefore, the geometry between camera heads can be considered a constant. The temporal geometric constraint introduced in this paper is that the relative position (X , Y , and Z) and relative orientation angles (ω , ϕ , and κ) between cameras heads are the same at different frames (different time instants). This condition can be used as additional observations in the bundle adjustment. Also, small movements or vibration can be considered by selecting proper weights to the constraint. The experiment results show that the temporal geometric constrained approach provides better results, in terms of accuracy as well as precision, than those of the bundle adjustment without constraints. The proposed approach can also be used for calibrating any multi-head camera system.

1. INTRODUCTION

An aerial multi-head camera system consists of multiple digital cameras that are mounted on a platform with different viewing angles, which maximizes ground coverage. At this time, a single digital camera cannot replace a film-based aerial mapping camera, due to technological and economical reasons (Tang et al., 2000). In the last decade, companies have introduced aerial digital mapping camera systems, which use multiple camera heads to overcome these problems. Aerial multi-head camera systems provide a single synthetic image from a set of images acquired simultaneously from each camera. To generate precise synthetic images, the EOP of each image should be precisely estimated. The EOP of each image can be calculated directly from navigation solutions and platform geometric calibration parameters. The platform geometric calibration parameters represent a geometric relationship between camera heads (Heier et al. 2002). To calculate precise EOP of the images acquired from each camera, the parameters should be precisely estimated. These parameters can be determined in a laboratory with a number of known control points (Gruber et al., 2008). However, if navigation solutions and platform calibration parameters are not available for some reason, the EOP of each image can be estimated by using ground control points (GCP). In this case, the geometric relationship between camera heads should be considered.

This paper introduces a bundle adjustment method with a temporal geometric constraint to estimate the precise EOP of images acquired from each camera of the aerial multi-head

camera system without navigation solutions and platform geometric calibration parameters. Each camera of the multi-head camera system is tightly affixed to the platform. Therefore, the geometry between camera heads can be considered a constant. The temporal geometric constraint introduced in this paper is that relative positions (X , Y , and Z) and relative orientation angles (ω , ϕ , and κ) between two cameras are the same at different frames. The temporal geometric constraint uses this condition as additional observations in the bundle adjustment.

(Di et al. 2004) used a constrained bundle adjustment to generate DEM from the images acquired from the rotating stereo camera system. The constraints used in this paper are the baseline and relative orientations with respect to the rotation center of the camera system. (Lee et al., 2010) introduced an in-flight platform geometric calibration method, which uses a temporal geometric constraint. The constraint used in this paper is that platform geometric calibration parameters are not changed at different frames. (Tomasselli et al., 2009) estimated camera calibration parameters using baseline and relative orientation constraints for the two-head camera system. In this paper, the distance between perspective centers of two cameras is used as a constraint for baseline. (Lerma et al., 2010) used a baseline distance constrained bundle adjustment for self calibration of the three-head camera system.

In this paper, the underlying mathematical models are outlined in Section 2, the experimental evaluations are described in Section 3, and the conclusion is discussed in Section 4.

2. MATHEMATICAL MODEL

2.1 Temporal geometric constraint

The temporal geometric constraint introduced in this paper is that the geometry between camera heads does not change over time. The term ‘temporal’ means that the constraint uses multiple frames, which are acquired at different time instants. The term ‘geometric’ means that the constraint uses geometry between images acquired at the same time instant.

The geometry between two camera heads can be expressed by three positional displacements and three rotation angles. Assume that two frames (frame 1 and 2) are acquired from a two-head camera system which consists of camera A and B. The coordinates of the perspective center of camera B in the coordinate system of camera A can be expressed by (1) and a rotation matrix from the coordinate system of camera A to the coordinate system of camera B can be expressed by (2).

$$\begin{bmatrix} X_{L_{AB}} \\ Y_{L_{AB}} \\ Z_{L_{AB}} \end{bmatrix} = M_A \left\{ \begin{bmatrix} X_{L_B} \\ Y_{L_B} \\ Z_{L_B} \end{bmatrix} - \begin{bmatrix} X_{L_A} \\ Y_{L_A} \\ Z_{L_A} \end{bmatrix} \right\} \quad (1)$$

$$M_{AB} = M_B M_A^T \quad (2)$$

where M_A , M_B are the rotation matrices of camera A and B, respectively. Subscript A and B refer to camera A and B, respectively.

Then, the temporal constraint is that the geometry between cameras A and B at frame 1 is identical to that of frame 2 and can be expressed by (3) and (4).

$$\begin{bmatrix} X_{L_{B_1}} - X_{L_{A_1}} \\ Y_{L_{B_1}} - Y_{L_{A_1}} \\ Z_{L_{B_1}} - Z_{L_{A_1}} \end{bmatrix} = \begin{bmatrix} X_{L_{B_2}} - X_{L_{A_2}} \\ Y_{L_{B_2}} - Y_{L_{A_2}} \\ Z_{L_{B_2}} - Z_{L_{A_2}} \end{bmatrix} \quad (3)$$

$$M_{AB} = M_{B_2} M_{A_2}^T = M_{B_1} M_{A_1}^T \quad (4)$$

where M_{A_1} , M_{A_2} are the rotation matrices of camera A at frame 1 and 2, respectively. $\begin{bmatrix} X_{L_{B_2}} \\ Y_{L_{B_2}} \\ Z_{L_{B_2}} \end{bmatrix}^T$ are the coordinates of the perspective center of camera B at frame 2. Subscript 1 and 2 refer to frames 1 and 2, respectively.

$$\begin{bmatrix} F \\ G \end{bmatrix} = \begin{bmatrix} M_{A_1} \\ M_{A_2} \end{bmatrix} \begin{bmatrix} X_{L_{A_1}} \\ Y_{L_{A_1}} \\ Z_{L_{A_1}} \end{bmatrix} - \begin{bmatrix} M_{A_2} \\ M_{A_1} \end{bmatrix} \begin{bmatrix} X_{L_{A_2}} \\ Y_{L_{A_2}} \\ Z_{L_{A_2}} \end{bmatrix} = \begin{bmatrix} 0 \\ 0 \end{bmatrix} \quad (5)$$

$$G = M_{B_2} M_{A_1}^T - M_{B_1} M_{A_2}^T = 0 \quad (6)$$

Linearized forms of (5) and (6) can be used as observations in a bundle adjustment. Each of two pairs of images provides six equations.

2.2 Bundle adjustment

Bundle adjustment is the most accurate method of triangulation and estimates all photogrammetric measurements simultaneously (Mikhail et al., 2001). The collinearity equations after linearization for a bundle adjustment can be found in (Mikhail et al., 2001) and (Wolf et al., 2000). The linearized form of the equations for bundle adjustment from (Mikhail et al., 2001) is repeated here in the interest of completeness (7).

$$v_{ij} + \hat{B}_{ij} \hat{\delta}_i + \hat{B}_{ij} \hat{\delta}_j = f_{ij} \quad (7)$$

where $\hat{\delta}_i$ contains corrections for the initial approximations of the EOP for image i , $\hat{\delta}_j$ contains corrections for the initial approximations of the object space coordinates of point j , \hat{B}_{ij} and \hat{B}_{ij} contain partial derivatives of the collinearity equations with respect to the EOP of image i and the object space coordinates of point j , respectively; f_{ij} contains the measured minus the estimated photo coordinates for point j on image i , and v_{ij} contains photo coordinate residuals.

The constraint equations that can be used as observations in the bundle adjustment can be expressed by equation (8). In this equation, subscript i, j, m, n refer to images. Image i and m are acquired from the same camera at different time instants. Images j and n are acquired from the same camera at different time instants. For example, image i and j are acquired from camera A and B at frame 1, and image m and n are acquired from camera A and B at frame 2.

$$v_{F_{ijmn}} + \hat{F}_i \hat{\delta}_i + \hat{F}_j \hat{\delta}_j + \hat{F}_m \hat{\delta}_m + \hat{F}_n \hat{\delta}_n = f_{F_{ijmn}} \quad (8)$$

$$v_{G_{ijmn}} + \hat{G}_i \hat{\delta}_i + \hat{G}_j \hat{\delta}_j + \hat{G}_m \hat{\delta}_m + \hat{G}_n \hat{\delta}_n = f_{G_{ijmn}} \quad (9)$$

where \hat{F}_i contains partial derivatives of the equation (5) with respect to the EOP of image i , \hat{G}_i contains partial derivatives of the equation (6) with respect to the EOP of image i ; $f_{F_{ijmn}}$ and $f_{G_{ijmn}}$ contain negative values of the estimated solutions of the equation (5) and (6), respectively, and $v_{F_{ijmn}}$ and $v_{G_{ijmn}}$ contain residuals.

The number of constraint equations can be calculated by (9). For example, three frames are acquired from a six-head camera system; the number of constraint equations is $15 \times 3 \times 6 = 270$.

$$c = \left(\sum_{i=1}^{n-1} 1 \right) \times \left(\sum_{j=1}^{m-1} 1 \right) \times 6 \quad (9)$$

where c is the number of constraint equations, n is the number of camera heads, and m is the number of frames.

The solution of the bundle adjustment can be obtained by solving the normal equation (10). The constraint equations can be included in the design matrix as observations. Proper weights should be given to the equations. Adjusting weights (W_F and W_G) can consider small movements of the camera heads.

$$\begin{bmatrix} \hat{N} \\ \hat{N} \\ \hat{N} \end{bmatrix} \begin{bmatrix} \hat{b} \\ \hat{b} \\ \hat{b} \end{bmatrix} = \begin{bmatrix} \hat{b} \\ \hat{b} \\ \hat{b} \end{bmatrix} \quad (10)$$

$$\begin{aligned} \hat{N} &= \hat{B}^T W \hat{B} + \hat{F}^T W_F \hat{F} + \hat{G}^T W_G \hat{G} + \hat{W} \\ \hat{N} &= \hat{B}^T W \hat{B} \\ \hat{N} &= \hat{B}^T W \hat{B} + \hat{W} \\ \hat{b} &= \hat{B}^T W \hat{f} + \hat{F}^T W_F \hat{f}_F + \hat{G}^T W_G \hat{f}_G - \hat{W} \hat{f} \\ \hat{b} &= \hat{B}^T W \hat{f} - \hat{W} \hat{f} \end{aligned}$$

where W , W , and W are the weight matrices for photo coordinate observations, ground control coordinate observations, and exterior orientation parameters, respectively. W_F and W_G are weight matrices for the constraint. \hat{f} and \hat{f} are total corrections to the original observations for the EOP and object coordinates, respectively.

3. EXPERIMENT

This section is dedicated to showing synthetic examples demonstrating the potential of the proposed approach. The synthetic dataset includes a six-head camera system, where each camera is oriented in such way as to maximize coverage. All six cameras of the system have the same specification. The focal lengths of all cameras are set to 50mm, the pixel size is $9\mu m \times 9\mu m$, and the size of image is 4096×2672 . Lens calibration parameters are known. Figure 1 illustrates designed geometry of the camera heads.

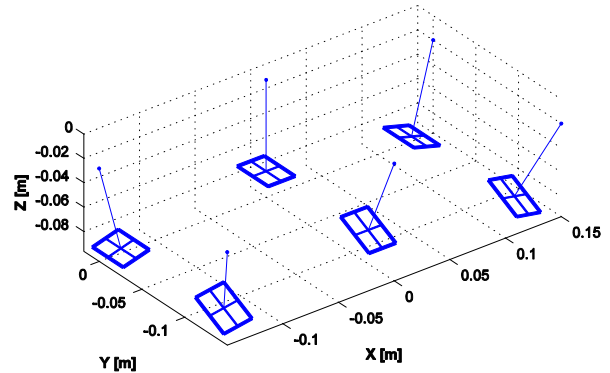


Figure 1. The geometry of the camera heads

Three synthetic target areas (sites A, B, and C) are generated for the tests. Each test has a different flying height and a different number of tie points (Table 1). For each data set, five GCPs with $\pm 0.5m$ precision in all X, Y, and Z directions are observed. Normally distributed random errors with ± 0.5 pixel ($\pm 4.5\mu m$) standard deviation are added to all photo coordinate measurements.

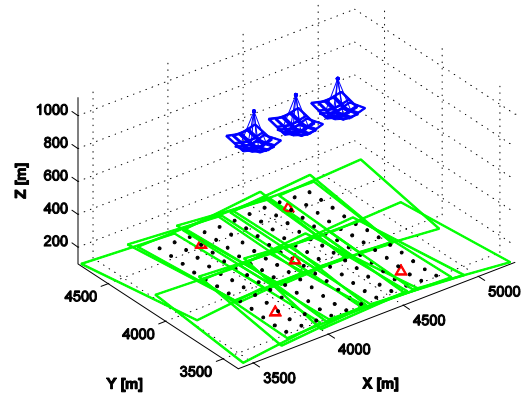


Figure 2. The geometry of the bundle adjustment for the test A

Test site	Flying height	Number of tie points
A	1010m	132
B	2000m	210
C	3000m	420

Table 1. Flying height and the number of tie points of test sites

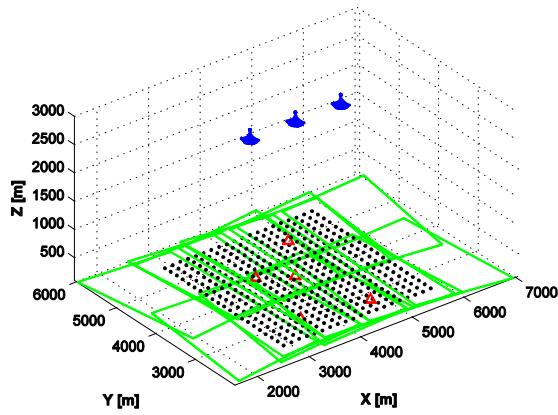


Figure 3. The geometry of the bundle adjustment for the test C

The average ground height of the target areas is approximately 100m. Images are acquired at three different time instants (three frames). Therefore, the number of total images acquired is $6 \times 3 = 18$. Overlaps between frames are around 60%. Figure 2 and 3 show the positions of the cameras (blue), ground coverage (green), GCPs (red), and tie points (black) for test sites A and C, respectively. In the figures, the focal length and size of each image are exaggerated for visualization.

$$\sigma_{\mu_x} = \pm \sqrt{\frac{\sum_{i=1}^n (X_i - \bar{X})^2}{n-1}} \quad (11)$$

Four types of bundle adjustments (no constraint, relative position constraint only, relative orientation angle constraint only, and position & angle constraint) are tested. To evaluate the performance of each method, the root mean square (RMS) residuals of check points, of which object coordinates are known but not used in the adjustment, were examined. RMS residuals for X direction can be calculated from (11).

Table 2 shows the comparison of the estimated variance of the unit weights and RMS residuals for the results of each method. RMS residuals and the estimated variance of unit weights of the proposed method (position & angle constraint) are smaller than those of other methods for all cases. According to the results of this comparison, it can be stated that the proposed method shows better results in terms of both precision and accuracy than the method without the constraint.

Test site (number of check points)	No constraint	Position constraint	Angle constraint	Position & angle constraint	
A (132)	$\sigma_{\mu_z}^2$	1.004431	0.886618	0.888251	0.792378
	μ_x	± 0.127 7m	± 0.1062 m	± 0.114 3m	± 0.101 4m
	μ_y	± 0.165 6m	± 0.1548 m	± 0.148 1m	± 0.138 1m
	μ_z	$\downarrow 0.423$ 9m	$\downarrow 0.3987$ m	$\downarrow 0.391$ 4m	$\downarrow 0.389$ 8m
B (151)	$\sigma_{\mu_z}^2$	0.995326	0.926011	0.927662	0.874552
	μ_x	± 0.134 9m	± 0.1250 m	± 0.125 2m	± 0.115 2m
	μ_y	± 0.183 8m	± 0.1748 m	± 0.177 3m	± 0.170 5m
	μ_z	± 0.525 2m	± 0.5123 m	± 0.509 0m	± 0.508 2m
C (81)	$\sigma_{\mu_z}^2$	1.014807	0.975263	0.978332	0.944584
	μ_x	± 0.152 8m	± 0.1513 m	± 0.143 0m	± 0.136 1m
	μ_y	± 0.229 6m	± 0.2235 m	± 0.216 2m	± 0.215 8m
	μ_z	$\downarrow 0.604$ 2m	$\downarrow 0.5879$ m	$\downarrow 0.580$ 6m	$\downarrow 0.578$ 2m

Table 2. The estimated variance of the unit weights and RMS residuals of the check points

4. CONCLUSION

This paper introduces a bundle adjustment method with a temporal geometric constraint for the multi-head camera system. If navigation solution and platform geometric calibration parameters are not available for some reason, the EOP of each image should be estimated using control points. The proposed approach introduces the temporal geometric constraint to acquire better adjustment results for this case. Each camera of the multi-head camera system is tightly fixed to the platform. Therefore, the geometry of the camera heads can be considered as a constant over time. The temporal geometric constraint uses this condition as additional observations in the bundle adjustment. The experiment results show that the temporal geometric constrained approach provides better results, in terms of accuracy as well as precision, than those of the bundle adjustment without constraints.

For the proposed method, weights can be selected for the relative position (X, Y, and Z) and relative orientation angles (ω , ϕ , and κ) between two camera heads independently. Therefore, only angular or positional movements can be considered. The proposed approach can also be used for calibrating any multi-head camera system.

REFERENCES

- Di, K., Xu, F., Li, R., 2004., Constrained bundle adjustment of panoramic stereo images for Mars landing site mapping, In: *Proceedings of the 4th International Symposium on Mobile Mapping Technology*, Kunming, China.
- Gruber, M., Ladstädter, R., 2008., Calibrating the digital large format aerial camera UltraCamX, In: *International Calibration and Orientation Workshop EuroCOW 2008 Proceedings*, Castelldefes, Spain.
- Heier, H., Kiefner, M., Zeitler, W., 2002., Calibration of the digital modular camera DMC, In: *FIG XXII International Congress*, Washington, D. C., USA.
- Lee, Y. J., Alper, Y., 2010., In-flight camera platform geometric calibration of the aerial multi-head camera system, In: *IEEE National Aerospace and Electronics Conference*, Dayton, USA.
- Lerma, J. L., Navarro, S., Cabrelles, M., 2010., Camera calibration with baseline distance constraints, *The Photogrammetric Record*, 25(130): pp. 140-158.
- Madani, M., Dörstel, C., Heipke, C. Jacobsen, K., 2004., DMC practical experience and accuracy assessment, In: *International Archives of Photogrammetry, Remote Sensing and Spatial Information Science*, (35), pp. 396-401.
- Mikhail, E. M., Bethel, J. S., McGlone, J. C., 2001. *Introduction to modern photogrammetry*, John Wiley & Sons, New York.
- Tang, L., Dörstel, C., Jacobsen, K., Heipke, C., Hinz, A., 2000. Geometric accuracy potential of the digital modular camera, In: *International Archives of Photogrammetry and Remote Sensing*, vol. XXXIII, Part B4/3, 2000, pp. 1051-1057.
- Tommaselli, A. M. G., Galo, M., Bazan, W. S., Ruy, R. S., Marcato Junior, J., 2009. Simultaneous calibration of multiple camera heads with fixed base constraint, In: *6th International Symposium on Mobil Mapping Technology*, Presidente Prudente, São Paulo, Brazil.
- Wolf, P. R., Dewitt, B. A., 2000, *Elements of Photogrammetry with Applications in GIS 3rd Edition*, McGraw-Hill, New York.